CHINESE OPTICS LETTERS

Vol. 21, No. 10 | October 2023

Stokes scintillations for vector beams in turbulence

Zhen Dong (董 震)[1], Bo Yuan (袁 波)[1], Yonglei Liu (刘永雷)[2], Fei Wang (王 飞)[1], Yangjian Cai (蔡阳健)[2*], and Yahong Chen (陈亚红)[1**]

[1] School of Physical Science and Technology, Soochow University, Suzhou 215006, China

[2] Shandong Provincial Engineering and Technical Center of Light Manipulations & Shandong Provincial Key Laboratory of Optics and Photonic Devices, School of Physics and Electronics, Shandong Normal University, Jinan 250014, China

*Corresponding author: yangjian_cai@163.com

**Corresponding author: yahongchen@suda.edu.cn

Received March 28, 2023 | Accepted May 18, 2023 | Posted Online August 22, 2023

We introduce the Stokes scintillation indices and the corresponding overall Stokes scintillations for quantitatively studying the fluctuations of both the intensity and polarization of an optical vector beam transmitting through the atmospheric turbulence. With the aid of the multiple-phase-screen method, we examine the Stokes fluctuations of a radially polarized beam in Kolmogorov turbulence numerically. The results show that the overall scintillation for the intensity distribution is always larger than the overall scintillation for the polarization-dependent Stokes parameters, which indicates that the polarization state of a vector beam is stabler than its intensity distribution in the turbulence. We interpret the results with the depolarization effect of the vector beam in turbulence. The findings in this work may be useful in free-space optical communications utilizing vector beams.

Keywords: Stokes scintillations; atmospheric turbulence; vector beams; polarization of light.
DOI: 10.3788/COL202321.100101

1. Introduction

Intensity scintillation index (SI) is a key metric in the free-space optical communication that measures the statistical property of the fluctuations induced in the intensity distribution of an optical beam by atmospheric turbulence[1]. Reducing the intensity SI is an important task in free-space optical communication applications[2]. To date, different types of approaches have been proposed to restrict the intensity scintillation, such as by using a stochastic electromagnetic beam, a beams array, and a partially coherent beam, as well as with the aid of adaptive optics[3–7]. Among others, the vector beams with spatially nonuniform polarization states[8], such as the cylindrical vector beams and fully Poincaré beams, have been shown to be useful, i.e., it was demonstrated that a vector beam has a lower intensity SI than that of its scalar modes (the modes with spatially uniform polarization states)[9–11].

However, as far as we know, all the research has focused only on the intensity fluctuations. The polarization property of a vector beam fluctuates as well in the turbulence[12], although it was shown only recently that the degree of vectorness remains unchanged during the vector beam propagating through the atmospheric turbulence[13]. Thus, how to describe quantitatively the fluctuations of the polarization property of a vector beam in turbulence becomes important, e.g., in free-space optical communications with the aid of vector beams[14–16].

For a fully polarized light, the polarization property can be described by the Jones vector. However, when a fully polarized beam propagates through a turbulent atmosphere, the beam becomes partially polarized due to the depolarization effect of the turbulence[17]. The Stokes parameters are widely used to describe the polarization properties of the partially coherent beams[18,19], including the polarization state of their fully polarized parts and the degree of polarization. In addition, the Stokes parameters are the real-valued quantities that can be obtained directly from several intensity measurements. Therefore, the fluctuations in the polarization property of a vector beam can be studied by measuring the statistical properties in the Stokes parameters.

To this end, in this work, we extend the intensity SI into four generalized Stokes SIs that describe the statistics of the fluctuations in the Stokes parameters of a vector beam. Meanwhile, we introduce the concept of overall Stokes scintillations to describe globally how stable the Stokes parameters within the beam's effective area are. As an example, we study the Stokes scintillations of a radially polarized beam propagating through an atmospheric turbulence obeying Kolmogorov statistics. It is found that the polarization-dependent Stokes parameters are stabler than the intensity distribution for the vector beam in turbulence. The findings are interpreted with the help of depolarization effect of the vector beam in the turbulence.

2. Stokes Scintillations

We start by considering a paraxial propagation vector beam along the z direction. Since its longitudinal field component can be neglected, only the two orthogonal transverse Cartesian components E_x and E_y need to be taken into account. The intensity and polarization properties of the beam, at a position $\mathbf{r}$ at frequency ω, are characterized by the four spectral Stokes parameters, which are defined as[20]

$$S_0(\mathbf{r},\omega) = E_x^*(\mathbf{r},\omega)E_x(\mathbf{r},\omega) + E_y^*(\mathbf{r},\omega)E_y(\mathbf{r},\omega), \tag{1}$$

$$S_1(\mathbf{r},\omega) = E_x^*(\mathbf{r},\omega)E_x(\mathbf{r},\omega) - E_y^*(\mathbf{r},\omega)E_y(\mathbf{r},\omega), \tag{2}$$

$$S_2(\mathbf{r},\omega) = E_x^*(\mathbf{r},\omega)E_y(\mathbf{r},\omega) + E_y^*(\mathbf{r},\omega)E_x(\mathbf{r},\omega), \tag{3}$$

$$S_3(\mathbf{r},\omega) = i[E_y^*(\mathbf{r},\omega)E_x(\mathbf{r},\omega) - E_x^*(\mathbf{r},\omega)E_y(\mathbf{r},\omega)]. \tag{4}$$

The four Stokes parameters are real-valued quantities that have clear physical interpretation, i.e., $S_0(\mathbf{r},\omega)$ represents the total intensity, while $S_1(\mathbf{r},\omega)$, $S_2(\mathbf{r},\omega)$, and $S_3(\mathbf{r},\omega)$ determine the polarization state of the vector beam.

When the vector beam propagates through a turbulent atmosphere, both the amplitude and phase of the beam's two orthogonal transverse field components suffer the turbulence perturbations, resulting in the random fluctuations in its Stokes parameters. The Stokes fluctuations, akin to the intensity fluctuation, are defined as

$$\Delta S_j(\mathbf{r},\omega) = S_j(\mathbf{r},\omega) - \langle S_j(\mathbf{r},\omega)\rangle, \tag{5}$$

with $j \in (0,1,2,3)$. $\Delta S_j(\mathbf{r},\omega)$ shows the fluctuations of the Stokes parameters around their average values. Above, $S_j(\mathbf{r},\omega)$ is a single realization of the Stokes parameters in the turbulence, while $\langle S_j(\mathbf{r},\omega)\rangle$ denotes its ensemble average. To quantitatively describe the Stokes fluctuations, we generalize the intensity SI and introduce the Stokes SIs, i.e.,

$$\sigma_j^2(\mathbf{r},\omega) = \frac{\langle[\Delta S_j(\mathbf{r},\omega)]^2\rangle}{\langle S_j(\mathbf{r},\omega)\rangle^2}. \tag{6}$$

The Stokes SIs measure the (normalized) variances of the Stokes fluctuations caused by atmospheric turbulence. Usually, the SIs increase with the growth of the turbulence strength. The smaller value for $\sigma_j^2(\mathbf{r},\omega)$ indicates higher stability of $S_j(\mathbf{r},\omega)$ in turbulence. We remark that $\sigma_0^2(\mathbf{r},\omega)$ shows the conventional intensity SI, which measures the intensity variance of the beam in turbulence. It is noted that the Stokes SIs have been proposed first for the partially coherent electromagnetic light beams due to the inherent random fluctuations in their sources[21]. Contrarily, in this work, we focus on the fluctuations of a fully coherent vector beam induced by the atmospheric turbulence.

Typically, in the spatial region where the energy of the beam tends to zero, a very small perturbation of turbulence will introduce a high value for $\sigma_j^2(\mathbf{r},\omega)$[9]. Thus, it is not convincing if we only study the scintillation indices at a single spatial position. In order to show the scintillations of the beam's Stokes parameters more effectively, we now introduce a global quantity that takes into account the Stokes scintillation indices at all the transverse spatial positions where the intensities are meaningful, i.e.,

$$\xi_j = \frac{1}{S_\Omega}\iint_\Omega \sigma_j^2(\mathbf{r},\omega)\mathrm{d}^2\mathbf{r}, \tag{7}$$

where Ω denotes the spatial region where the intensity of the beam is effective and S_Ω is the area of Ω. We term the quantity ξ_j as the overall Stokes scintillations. It is remarkable that in the above definition the nonnegative nature of the Stokes scintillation indices is used.

3. Simulations

In the following, we use the above general formulas to study the stability of the intensity and polarization of a vector beam passing through an atmospheric turbulence. In the simulation, we consider a radially polarized beam with its electric field that can be written as a superposition of the optical modes at two poles of a higher-order Poincaré sphere[22], i.e.,

$$\mathbf{E}(\mathbf{r}) = \mathrm{LG}_{0,+1}(\mathbf{r})\hat{\mathbf{e}}_R + \mathrm{LG}_{0,-1}(\mathbf{r})\hat{\mathbf{e}}_L, \tag{8}$$

where $\mathrm{LG}_{0,l}(\mathbf{r}) = \sqrt{\frac{2}{\pi|l|!}}\left(\frac{\sqrt{2}r}{\omega_0}\right)^{|l|}L_0^{|l|}\left(\frac{2r^2}{\omega_0^2}\right)\exp\left(-\frac{r^2}{\omega_0^2}\right)\exp(il\varphi)$ is a Laguerre–Gaussian mode with $l = \pm 1$ for the radially polarized beam. Above, $L_0^{|l|}(\cdot)$ is the generalized Laguerre polynomial, ω_0 is the beam waist, and (r,φ) is the polar coordinate. $\hat{\mathbf{e}}_R$ and $\hat{\mathbf{e}}_L$ are the unit vectors for the right- and left-handed circular polarization states, respectively. The atmospheric turbulence is assumed to obey Kolmogorov statistics and the van Kármán power spectrum for the index-of-refraction fluctuations is adopted[17], i.e.,

$$\Phi_n(\kappa) = 0.033C_n^2(\kappa^2 + \kappa_0^2)^{-11/6}\exp(-\kappa^2/\kappa_m^2), \tag{9}$$

where C_n^2 is a generalized refractive-index structure parameter, $\kappa = \sqrt{\kappa_x^2 + \kappa_y^2}$ with $(\kappa_x,\ \kappa_y)$ being the spatial frequency vector, and $\kappa_0 = 2\pi/T_0$ and $\kappa_m = 5.92/t_0$ with T_0 and t_0 being the outer and inner scale of the turbulence.

3.1. Multiple-phase-screen method

The propagation of the radially polarized beam through the Kolmogorov turbulence is solved with the help of the multiple-phase-screen method[23,24], in which the turbulence is modeled as a collection of thin random phase screens with the desired turbulence statistics. The random phase screens are placed along the transmission path at equal intervals $\Delta z = z/M$, where Δz is the distance between two adjacent phase screens, z is the length of the turbulence link, and M denotes the total number of the random phase screens. As shown in Fig. 1, the incident radially polarized beam first propagates a distance

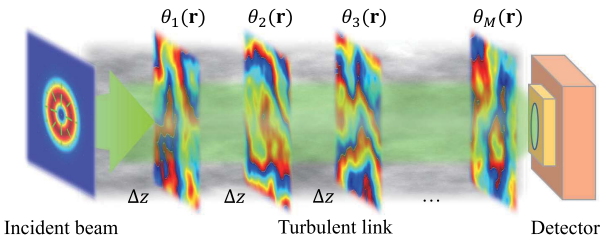

Fig. 1. Schematic diagram illustrating the propagation of a radially polarized beam through a turbulent atmosphere in terms of the multiple-phase-screen method.

Δz in free space and arrives at the first phase screen. The electric field in the plane of the phase screen is modified by a random phase $\theta_1(\mathbf{r})$, which represents the accumulated turbulence effect over Δz. The above step is repeated until the beam reaches the last phase screen, and finally, the light beam arrives at the detector, which records a single realization of the field (or an instantaneous field). Another realization is obtained by refreshing the phase screens and propagating the radially polarized beam through the path again. In our simulation, 600 realizations are obtained to calculate the average Stokes parameters.

The random phase $\theta_m(\mathbf{r})$ for the mth phase screen is obtained by

$$\theta_m(\mathbf{r}) = \mathrm{Re}\left\{\mathcal{F}[\sqrt{2\pi\Delta z k^2 \Phi_n(\kappa)} R_m(\kappa)]\right\}, \tag{10}$$

where Re denotes the real part, $\mathcal{F}$ denotes the Fourier transform, $k = 2\pi/\lambda$ is the wavenumber (λ the wavelength), and the function $R_m(\kappa)$ is a complex Gaussian random function with both its real and imaginary parts having the unit variance and zero mean. In the multiple-phase-screen method, the turbulence within the range of Δz should be weak; that is to say, the range Rytov variance $\sigma_r^2 = 1.23 C_n^2 k^{7/6} \Delta z^{11/6} < 0.1$. Moreover, σ_r^2 should be less than 10% of the total Rytov variance $\sigma_R^2 = 1.23 C_n^2 k^{7/6} z^{11/6}$ within the whole z range. In our simulation, the length of the turbulence channel is fixed to 1000 m, and $M = 16$ phase screens are used. The outer and inner scales of the turbulence are $T_0 = 3$ m and $t_0 = 1$ mm. The strength of the turbulence is determined by σ_R^2. For weak turbulence $\sigma_R^2 < 1$, while for moderate and strong turbulences, $\sigma_R^2 \geq 1$. In our simulation, σ_R^2 varies from 0.1 to 5. The wavelength and the beam waist of the incident beam are $\lambda = 532$ nm and $\omega_0 = 2$ cm, respectively. The conditions for the multiple-phase-screen method are satisfied with the above parameters.

3.2. Simulation results

The top panels of Fig. 2 show the simulation results for the intensity $S_0(\mathbf{r})$ and the polarization state [obtained by $S_1(\mathbf{r})$, $S_2(\mathbf{r})$, and $S_3(\mathbf{r})$] of each single realization in the receive plane when the radially polarized beam passes through the turbulence link with $\sigma_R^2 = 0.1$ and $\sigma_R^2 = 1$. The corresponding results for the average intensity $\langle S_0(\mathbf{r})\rangle$ and polarization state, as well as the degree of

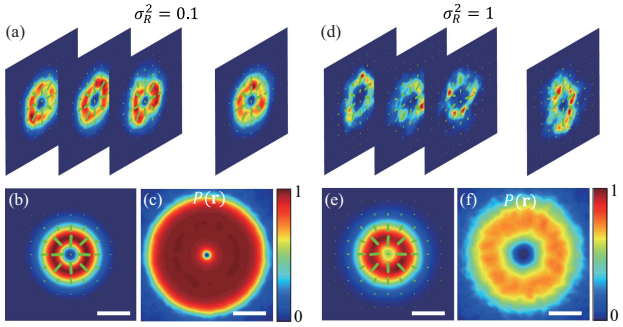

Fig. 2. Simulation results for the intensity and polarization state of (a), (d) the instantaneous field realizations and (b), (e) the averaged field over 600 realizations in the receive plane after the radially polarized beam passing through the atmospheric turbulence; (c) and (f) show the degree of polarization $P(\mathbf{r})$ of the averaged field. In (a)–(c), $\sigma_R^2 = 0.1$, while in (d)–(f), $\sigma_R^2 = 1$. The scale bar is 3 cm.

polarization $P(\mathbf{r}) = \sqrt{\sum_{j=1}^{3} \langle S_j(\mathbf{r})\rangle^2} / \langle S_0(\mathbf{r})\rangle$[20] are presented in the bottom panels of Fig. 2. It is found that the radially polarized beam is unaffected by the weak turbulence with $\sigma_R^2 = 0.1$ [Fig. 2(a)]. When the turbulence strength increases to $\sigma_R^2 = 1$, we find both the intensity and the polarization state of the instantaneous field become unstable [Fig. 2(d)], resulting in the degeneration of the dark-hollow distribution in the average intensity [see Fig. 2(e)]. The dark cone in the average intensity disappears because of the depolarization effect of the beam induced by the turbulence fluctuations. As shown in Figs. 2(c) and 2(f), the degree of polarization of the average beam reduces with the increasing turbulence strength. It is worth noting that the instantaneous field for a single realization still remains essentially fully polarized. In contrary to the average intensity, it is found that the polarization state of the average beam is less affected by the turbulence fluctuations, i.e., in Figs. 2(b) and 2(e), the beam still shows a fine radial polarization distribution.

Figures 3(a)–3(d) show the spatial distributions for the instantaneous Stokes parameters of one single realization, while Figs. 3(e)–3(h) display the average Stokes parameters over $N = 600$ realizations for the case when $\sigma_R^2 = 1$. Compared to the three polarization-dependent Stokes parameters, we find the intensity fluctuation $\Delta S_0(\mathbf{r})$ is larger than the polarization-dependent Stokes fluctuations. Based on Eq. (6), we obtain the spatial distributions of the corresponding Stokes SIs, which are shown in Figs. 3(i)–3(l). We find that outside the white dashed ring (where the average intensity is less than 10% of its maximum value) the SIs are much higher than those inside the ring. However, these highly valued indices outside the ring cannot correctly reflect the Stokes fluctuations of the beam, since at those positions the beam has negligible power, as shown in Fig. 3(e). Thus, we only take the Stokes SIs inside the ring into account, and we calculate the overall Stokes scintillations with the help of Eq. (7). The calculated values for the four overall Stokes scintillations are presented in Fig. 3(m). First, we find the overall intensity scintillation $\xi_0 = 0.96$ is higher than the polarization-dependent

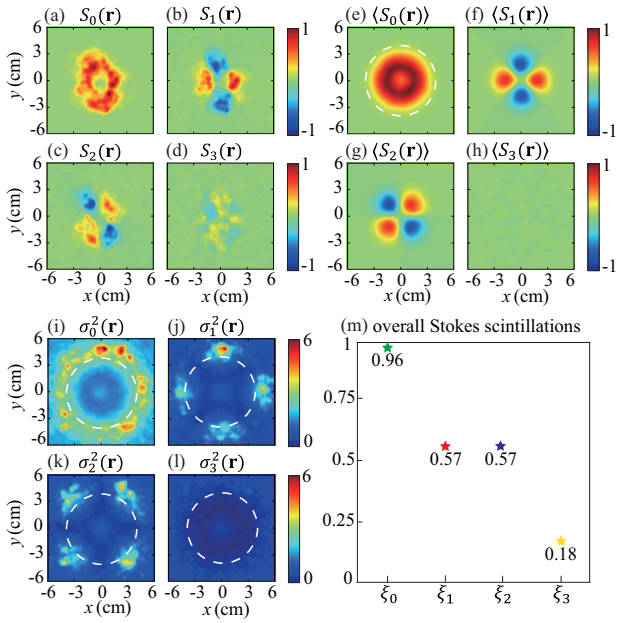

Fig. 3. Spatial distributions for (a)–(d) the instantaneous Stokes parameters of a single realization; (e)–(h) the average Stokes parameters over 600 realizations; and (i)–(l) the Stokes scintillation indices in the receive plane after the radially polarized beam passing through the atmospheric turbulence with σ_R^2 = 1. (m) shows the calculated values for the four overall Stokes scintillations. In (e) and (i)–(l), within the white dashed ring the average intensity is larger than 10% of its maximum value.

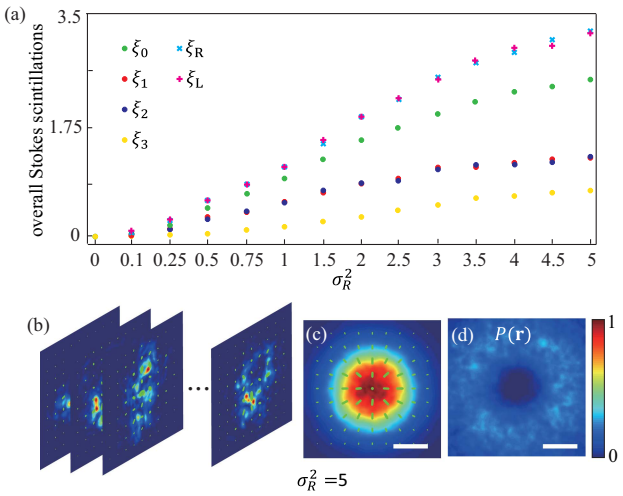

Fig. 4. (a) Behavior of overall Stokes scintillations with the Rytov variance σ_R^2 for the radially polarized beam propagation through the atmospheric turbulence; simulation results for the intensity and polarization state of (b) the instantaneous field realizations and (c) the averaged field over 600 realizations in the receive plane for σ_R^2 = 5; (d) shows the degree of polarization of the averaged field. The overall intensity scintillations ξ_R and ξ_L for the scalar modes $\mathrm{LG}_{0,+1}(\mathbf{r})\hat{\mathbf{e}}_R$ and $\mathrm{LG}_{0,-1}(\mathbf{r})\hat{\mathbf{e}}_L$ are also shown in (a). The scale bar is 3 cm.

overall Stokes scintillations ξ_1, ξ_2, and ξ_3, which indicate that the polarization-dependent Stokes parameters are stabler than the intensity for a radially polarized beam in the turbulence. It is also found that $\xi_1 = \xi_2 = 0.57$. This is because of the symmetric spatial distributions of $S_1(\mathbf{r})$ and $S_2(\mathbf{r})$ for the radially polarized beam, i.e., by rotating $S_1(\mathbf{r})$ 45 deg counterclockwise, $S_2(\mathbf{r})$ is obtained. The smallest value for ξ_3 is due to the appearance of the circular polarization in the instantaneous field realizations, as shown in Figs. 2(d) and 3(d). It should be noted that there is effectively no circular polarization in the averaged field [Fig. 2(e)], which can also be seen from Fig. 3(h) that $\langle S_3(\mathbf{r})\rangle$ nearly vanishes.

To examine the effect of turbulence strength on the overall Stokes scintillations, we plot in Fig. 4(a) the behavior of ξ_0, ξ_1, ξ_2, and ξ_3 with different turbulence strengths. It is found that with the increase of σ_R^2, all the four overall Stokes scintillations increase as well. When $\sigma_R^2 = 5$, the values of overall Stokes scintillations are about twice as large as those in the case when $\sigma_R^2 = 1$. The intensity and polarization state of instantaneous field realizations and their average field are shown in Figs. 4(b) and 4(c), respectively. Compared to the instantaneous intensity and polarization state shown in Fig. 2, we find the beam indeed becomes more unstable with the increase of overall Stokes scintillations. From Fig. 4(a), we also find that the intensity overall scintillation ξ_0 (green dots) is always greater than the polarization-dependent overall Stokes scintillations (except for the beam in free space with $\sigma_R^2 = 0$). In addition, with the increase of the turbulence strength the gaps between these overall scintillations enlarge, which indicates that the polarization-dependent Stokes parameters of a vector beam are stabler compared to the intensity distribution; this effect is more obvious when the turbulence strength increases.

Meanwhile, it is found in Fig. 4(a) that, the same as the case for $\sigma_R^2 = 1$, $\xi_1 = \xi_2$ holds for other turbulence strengths, indicating that the symmetric property in $\langle S_1(\mathbf{r})\rangle$ and $\langle S_2(\mathbf{r})\rangle$ is almost unaffected by the turbulence, which therefore determines that the radial polarization state of the averaged field is less affected by the turbulence [see Figs. 2(b), 2(e), and 4(c)]. The spatial distributions of $\langle S_1(\mathbf{r})\rangle$ and $\langle S_2(\mathbf{r})\rangle$ maintained in the turbulence indicate that the vector polarization state is stable. Thus, the similar conclusions can be obtained with other polarization representations, such as the recently proposed four-parameter notation[25]. Moreover, we plot in Fig. 4(a) the intensity overall scintillations ξ_R and ξ_L for the scalar modes $\mathrm{LG}_{0,+1}(\mathbf{r})\hat{\mathbf{e}}_R$ and $\mathrm{LG}_{0,-1}(\mathbf{r})\hat{\mathbf{e}}_L$ that construct the radially polarized beam. It is found that $\xi_R = \xi_L$, and they are always larger than the overall intensity scintillation ξ_0 for the radially polarized beam, which is consistent with the conclusion that a vector beam has a smaller intensity SI than its scalar modes in the turbulence obtained before[9]. We note the slight difference between ξ_R and ξ_L is due to the simulation accuracy for the multiple-phase-screen method. With the increase of the turbulence realizaitons, the simulation error will be decreased as well.

3.3. Interpretation with depolarization effect

The increased gaps between overall scintillations can be explained with the help of the degree of polarization. From

Figs. 2(c), 2(f), and 4(d), we find with the increase of the turbulence strength, the degree of polarization $P(\mathbf{r})$ of the averaged beam in the receive plane decreases, similar to depolarization in turbid water[26]. Thus, the intensity of the beam contains both the polarized part and unpolarized part. In other words, the intensity is affected by the fluctuations of both the polarized and unpolarized parts, while the polarization-dependent Stokes parameters are affected only by the fully polarized part. As a result, the overall intensity scintillation is always larger than the polarization-dependent overall Stokes scintillations when the beam becomes partially polarized after the turbulence. To show the depolarization effect more intuitively, we show in Fig. 5 the behavior of the normalized power for the fully polarized and completely unpolarized parts of the beam with different turbulence strengths. The normalized power is defined as

$$\eta_j = \frac{\iint_\Omega I_j(\mathbf{r})\mathrm{d}^2\mathbf{r}}{\iint_\Omega I(\mathbf{r})\mathrm{d}^2\mathbf{r}}, \tag{11}$$

where $j \in (p, u)$ denotes the polarized and unpolarized part, and $I_p(\mathbf{r})$, $I_u(\mathbf{r})$, and $I(\mathbf{r})$ are the intensities for the polarized part, unpolarized part, and the total intensity, respectively. We find from Fig. 5 that with the increase of the turbulence strength, the beam power in the fully polarized part generally transmits to the unpolarized part. For the relatively weak turbulence, the beam is constituted mainly by the fully polarized part, and therefore the gaps between the overall scintillations are small, while for the stronger turbulence, the unpolarized part becomes dominant, and thus the gaps become large. The depolarization effect is also shown in the average intensity in the receive plane; see Figs. 2(b), 2(e), and 4(c). With the increase of the turbulence strength, the beam becomes less polarized, and its beam profile gradually changes from dark-hollow to Gaussian distribution. This is because the intensity $I_p(\mathbf{r})$ for the fully polarized part shows the dark-hollow profile, while the intensity $I_u(\mathbf{r})$ for the unpolarized part shows the Gaussian distribution. With the increase of the turbulence strength, the Gaussian-shaped unpolarized part will become dominant.

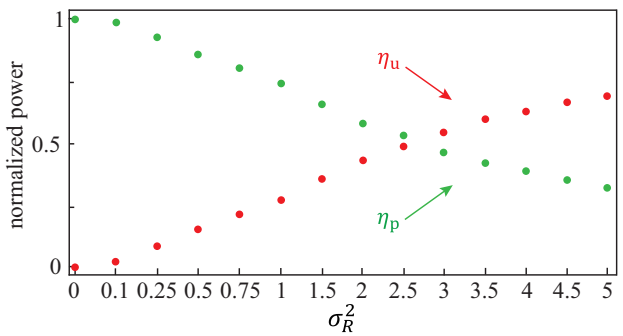

Fig. 5. Behavior of normalized power for the fully polarized part (η_p) and the completely unpolarized part (η_u) of the beam with the Rytov variance σ_R^2.

4. Conclusions

In summary, we have examined the statistical properties for the Stokes parameters fluctuations of a radially polarized beam propagating in atmospheric turbulence. To this end, we extended the concept of intensity SI into four generalized Stokes SIs and introduced the overall Stokes scintillations to show globally the stability of the Stokes parameters within the effective beam's area. The simulation results obtained with the multiple-phase-screen method showed that the overall scintillation for the intensity is always greater than those for the polarization-dependent Stokes parameters, and the gaps between these overall scintillations increase with enhancing the turbulence strength, which indicates that the polarization-dependent Stokes parameters of a vector beam are stabler than its intensity distribution in the turbulence. The results have been interpreted with the depolarization effect of the vector beam in the turbulence. We remark that the obtained conclusions in this work are valid also for the vector beams with higher-order polarization states (i.e., the polarization order $l > 1$). We expect that our findings may find use in light-polarization-based free-space optical communications.

Acknowledgement

This work was supported by the National Key Research and Development Program of China (Nos. 2022YFA1404800 and 2019YFA0705000), the National Natural Science Foundation of China (Nos. 11874046, 12192254, 92250304, 11974218, 11904247, 12174279, 12274310, and 12274311), and the Local Science and Technology Development Project of the Central Government (No. YDZX20203700001766).

References

1. L. C. Andrews, R. L. Phillips, and C. Y. Hopen, *Laser Beam Scintillation with Applications* (SPIE, 2001).
2. H. Kaushal and G. Kaddoum, "Optical communication in space: challenges and mitigation techniques," IEEE Commun. Surv. Tutor. **19**, 57 (2016).
3. O. Korotkova, "Scintillation index of a stochastic electromagnetic beam propagating in random media," Opt. Commun. **281**, 2342 (2008).
4. Y. Gu and G. Gbur, "Scintillation of Airy beam arrays in atmospheric turbulence," Opt. Lett. **35**, 3456 (2010).
5. F. Wang, Y. Cai, H. T. Eyyuboğlu, and Y. Baykal, "Twist phase-induced reduction in scintillation of a partially coherent beam in turbulent atmosphere," Opt. Lett. **37**, 184 (2012).
6. W. S. Rabinovich, R. Mahon, M. Ferraro, P. G. Goetz, and J. L. Murphy, "Reduction of scintillation in optical modulating retro-reflector links," Opt. Express **22**, 28553 (2014).
7. Y. Baykal, "Adaptive optics correction of scintillation in underwater medium," J. Mod. Opt. **67**, 220 (2020).
8. Z. Li, Y. Ruan, P. Chen, J. Tang, W. Hu, K. Xia, and Y. Lu, "Liquid crystal devices for vector vortex beams manipulation and quantum information applications [Invited]," Chin. Opt. Lett. **19**, 112601 (2021).
9. Y. Gu, O. Korotkova, and G. Gbur, "Scintillation of nonuniformly polarized beams in atmospheric turbulence," Opt. Lett. **34**, 2261 (2009).
10. S. Avramov-Zamurovic, C. Nelson, R. Malek-Madani, and O. Korotkova, "Polarization-induced reduction in scintillation of optical beams propagating in simulated turbulent atmospheric channels," Waves Complex Random Media **24**, 452 (2014).

11. C. Wei, D. Wu, C. Liang, F. Wang, and Y. Cai, "Experimental verification of significant reduction of turbulence-induced scintillation in a full Poincaré beam," Opt. Express **23**, 24331 (2015).
12. W. Cheng, J. W. Haus, and Q. Zhan, "Propagation of vector vortex beams through a turbulent atmosphere," Opt. Express **17**, 17829 (2009).
13. I. Nape, K. Singh, A. Klug, W. Buono, C. Rosales-Guzman, A. McWilliam, S. Franke-Arnold, A. Kritzinger, P. Forbes, A. Dudley, and A. Forbes, "Revealing the invariance of vectorial structured light in complex media," Nat. Photonics **16**, 538 (2022).
14. G. Milione, M. P. J. Lavery, H. Huang, Y. Ren, G. Xie, T. A. Nguyen, E. Karimi, L. Marrucci, D. A. Nolan, R. R. Alfano, and A. E. Willner, "4× 20 Gbit/s mode division multiplexing over free space using vector modes and a *q*-plate mode (de)multiplexer," Opt. Lett. **40**, 1980 (2015).
15. M. A. Cox, C. Rosales-Guzmán, M. P. J. Lavery, D. J. Versfeld, and A. Forbes, "On the resilience of scalar and vector vortex modes in turbulence," Opt. Express **24**, 18105 (2016).
16. Z. Zhu, M. Janasik, A. Fyffe, D. Hay, Y. Zhou, B. Kantor, T. Winder, R. W. Boyd, G. Leuchs, and Z. Shi, "Compensation-free high-dimensional free-space optical communication using turbulence-resilient vector beams," Nat. Commun. **12**, 1666 (2021).
17. L. C. Andrews and R. L. Phillips, *Laser Beam Propagation through Random Media*, 2nd ed. (SPIE, 2005).
18. C. Brosseau, *Fundamentals of Polarized Light: A Statistical Optics Approach* (Wiley, 1998).
19. Z. Dong, Y. Chen, F. Wang, Y. Cai, A. T. Friberg, and T. Setälä, "Encoding higher-order polarization states into robust partially coherent optical beams," Phys. Rev. Appl. **18**, 034036 (2022).
20. L. Mandel and E. Wolf, *Optical Coherence and Quantum Optics* (Cambridge University, 1995).
21. D. Kuebel and T. D. Visser, "Generalized Hanbury Brown-Twiss effect for Stokes parameters," J. Opt. Soc. Am. A **36**, 362 (2019).
22. G. Milione, H. I. Sztul, D. A. Nolan, and R. R. Alfano, "Higher-order Poincaré sphere, Stokes parameters, and the angular momentum of light," Phys. Rev. Lett. **107**, 53601 (2011).
23. J. M. Martin and S. M. Flatté, "Intensity images and statistics from numerical simulation of wave propagation in 3-D random media," Appl. Opt. **27**, 2111 (1988).
24. L. Zhao, Y. Hao, L. Chen, W. Liu, M. Jin, Y. Wu, J. Tao, K. Jie, and H. Liu, "High-accuracy mode recognition method in orbital angular momentum optical communication system," Chin. Opt. Lett. **20**, 020601 (2022)
25. S. Fu, L. Hai, R. Song, C. Gao, and X. Zhang, "Representation of total angular momentum states of beams through a four-parameter notation," New J. Phys. **23**, 083015 (2021).
26. F. Liu, S. Zhang, P. Han, F. Chen, L. Zhao, Y. Fan, and X. Shao, "Depolarization index from Mueller matrix descatters imaging in turbid water," Chin. Opt. Lett. **20**, 022601 (2022).